

## Research Article

# Estimation of Fracture Size and Probability Density Function by Setting Scanlines in Rectangular Sampling Window

Feifan Gu,<sup>1</sup> Jianping Chen,<sup>1</sup> Qi Zhang,<sup>2</sup> Chun Tan,<sup>3,4</sup> Yansong Zhang,<sup>1</sup> and Qing Wang<sup>1</sup>

<sup>1</sup>College of Construction Engineering, Jilin University, Changchun, Jilin 130026, China

<sup>2</sup>Northeast Electric Power Design Institute Co., Ltd., Changchun, Jilin 130026, China

<sup>3</sup>China Water Northeastern Investigation, Design and Research Co., Ltd, Changchun, Jilin 130026, China

<sup>4</sup>North China Power Engineering Co., Ltd. of China Power Engineering Consulting Group, Changchun, Jilin 130000, China

Correspondence should be addressed to Qing Wang; wangqing@jlu.edu.cn

Received 2 November 2022; Accepted 7 September 2023; Published 8 November 2023

Academic Editor: Songjian Ao

Copyright © 2023. Feifan Gu et al. Exclusive Licensee GeoScienceWorld. Distributed under a Creative Commons Attribution License (CC BY 4.0).

Rock masses are very important materials in geotechnical engineering. In engineering rock mass, fracture is the relatively weak part of mechanical strength in rock mass and is the most important factor controlling the deformation, damage, and permeability of rock mass. Therefore, investigating fractures is very important for characterizing rock mass. This paper proposed a new approach by using uniformly equidistant orthogonal scanlines. Within the study context, the solution formula of fracture size is derived by establishing the space intersection model of arbitrary fracture and scanline, rectangular window, and a rectangular box with a rectangular window. Then, fractures were randomly generated in a certain size cube and compared with the traditional Kulatilake trace length integral evaluation method. The study results have shown that the proposed method is more reasonable and accurate. Then, this method was applied to an adit of Songta Hydropower Station. Finally, a new fracture diameter probability density estimation method was proposed, the fracture diameter of the normal distribution was verified, and the parameters of the probability density function obtained by the scanlines method were in agreement with the initial set parameters. In summary, the proposed scanlines method can well estimate the mean value of the fracture diameter and the probability density function of the fracture size.

## 1. Introduction

Typically, the rock mass has three characteristics caused by their fractures, anisotropy, pleiotropy, and heterogeneity [1]. Fracture properties can significantly influence the behavior of the rock mass in many ways, including strength, deformation, stress-strain relation, permeability, and failure. These properties mainly include fracture orientation, density, size, surface features (such as infill material, roughness, and fracture opening), and persistence ratio [2]. Therefore, it is necessary to investigate and analyze fractures in the rock mass, but in practical rock engineering and field survey, only the orientation, trace length, location, and surface features of fractures can be directly

obtained. Based on this information, a three-dimensional fracture network (DFN) can be established, which is widely used in hydraulic, hydropower, mining, and nuclear power engineering. Indeed, the estimation of fracture size is an important part for DFN model and is also the main focus of this paper.

A fracture is a planar two-dimensional geological surface in three-dimensional space. At present, the actual shape of fractures in space is still unknown, and the actual fracture size cannot be obtained. Robertson [3] put forward that the fracture length in the strike direction was basically the same as that in the dip direction by the field survey of 9000 fractures in South African iron mine and highlighted that the fracture was

a thin disk in space. Later this viewpoint was accepted and adopted by many scholars [4]. Barton [5] thought that the spatial shape of fracture was elliptical. Glynn et al. presented that it was more reasonable to apply the Poisson surface as the geometry of the fracture in space [6, 7]. Some scholars thought that the geometry of spatial fracture could also be polygons such as rectangle, parallelogram, diamond, and triangle. However, the viewpoint that the fracture is a thin disk in space is widely used and applied as the fundamental assumption. Currently, the fracture shape is divided into three types: (1) Fracture orthogonal model, which was first proposed by He et al. [8] in 1995 to calculate fracture spacing more conveniently. This model assumed that all fractures could be divided into three parallel groups. (2) Beaeher disk model, which was established by Beaeher et al. in 1978. This model was later widely used by scholars [9]. The joint shape in this model is described as a circle, and the position of the fracture surface is determined by the spatial coordinates ( $x$ ,  $y$ , and  $z$ ) of the disk's center. The dip and dip angle of the fracture are determined through the angle of the disk relative to the rectangular coordinate system  $\alpha$  and  $\beta$ . The size of the fracture is determined by the radius  $r$  of the disk. (3) Polygonal model, which was first presented by Veneziano [10] in 1978. Veneziano thought that the fracture shape in space is polygonal, but he did not consider the intersection points when polygonal fractures intersect. Based on the imperfection of the Veneziano model, Dershowitz improved the model in 1984 [11]. There are also some other fracture models. Zheng et al. [12] and Guo et al. [13] proposed the universal elliptical disc model and applied it to the establishment of the three DFN model of the actual slope engineering. The results show that compared with the disk model and the nonuniversal elliptical disk model, the universal elliptical disc model has a better simulation effect on rock slope, especially for the modeling process of slender natural fractures. In the establishment of three DFN model, fractures are usually considered thin disk or circular fractures whose center points obey Poisson distribution. This study regards the fracture as a thin disk.

In general, fracture size cannot be directly measured, but it can be indirectly calculated by establishing the relationship between the three-dimensional fracture size and the two-dimensional trace length in the sampling window. Kendall and Moran [14] proposed the relationship between the probability density function of intersecting trace length distribution when fracture size was constant in 1963, but this method assumed that fracture size in space was constant, which is obviously contrary to engineering practice. Kulatilake [15] assumed that the center point of fracture was evenly distributed in space, and fracture diameter and orientation were independent. Based on this assumption, Kulatilake presented a method for estimating fracture disk diameters and probability density functions by trace length. This method was a more classical method and was widely accepted and applied by scholars, but it depends greatly on the accuracy of the measurement and fitting

distribution function of trace length. Hence, its results were unstable. Song [16] estimated the probability density function of the fracture diameter based on the endpoints of the trace. This method was a distribution-free estimation method, which was suitable for any shape of fractures such as circles, rectangles, ellipses, and other polygons. Zhu Hehua proposed a distribution-free method for estimating the fracture diameter distribution using moments in conjunction with the maximum entropy principle. The method of the maximum entropy principle could achieve a universal form for the fracture diameter distribution without any particular form [17]. Gao Mingzhong [18] presented an estimation method of fracture size using data sampled from boreholes, assuming that the fracture was elliptical. The mean fracture size and standard deviation were calculated by considering the number of intersections between the fractures and the boreholes.

According to the distribution of all traces in the rectangular window, Zhang [19] covered the window with uniform and equidistant orthogonal grids, took the grid lines as survey lines, estimated the trace length mean value, verified the new method by randomly generating the trace length data of fracture, and applied it to specific engineering practice. At the same time, he proposed a new method for fitting the trace length probability density function. In this paper, rectangular windows are also covered by uniform and equidistant orthogonal grids, and the space model of intersection between fracture and survey line, the space model of intersection between fracture and rectangular window, and the space model of intersection between fracture and rectangular window are, respectively, established by applying the principle of probability statistics to calculate the mean value of fracture diameter. Finally, based on the assumption that the probability density function of disk diameter is the same as that of the two-dimensional full trace length, a new method for estimating the probability density of disk diameter is proposed.

## 2. Mathematical Model

In practical rock engineering and field surveys, only the orientation, trace length, location, and surface features of fractures can be directly obtained. Among them, trace length is important for the estimation of fracture size. There are three widely used methods for measuring the trace length [20], which can be summarized as follows: (1) scanline survey by measuring the trace length intersected with scanlines [21], (2) window sampling by measuring the trace length within a finite area [22, 23], and (3) circle sampling by measuring the trace length intersected with a circle [24]. Most methods have dimension deviation and truncation error because there are three intersecting states between trace length and sampling window: (a) both ends observable, (b) only one end observable, and (c) both ends censored, as shown in Figure 1. Assume that  $N_0$  are the fractures whose both ends are censored,  $N_1$  are the fractures whose one end is observable and another end is censored,  $N_2$  are the fractures whose both ends are observable, and  $N$

are the total fractures in the sampling window, then  $N=N_0 + N_1 + N_2$ . We can further calculate  $R_0 = N_0/N$ ,  $R_1 = N_1/N$ , and  $R_2 = N_2/N$ .

The trace length and size of the fracture diameter are two different concepts, but they are closely related. The trace length is the length of the intersection line between the fracture diameter and the natural outcrop or the artificial excavation surface, and the size of the fracture diameter is its extension feature in the three-dimensional space. Assuming that the fracture diameter is a thin disk, there is a certain probability relationship model between the track length and the disk diameter. Therefore, the average value and probability distribution of the disk diameter can be inferred from the track length and its distribution. Warburton [25] came up with the idea of estimating the diameter based on the full trace length of the outcrop and derived the implicit functional relationship between the full trace length of the outcrop and the diameter distribution. Priest and Hudson [26] obtained the relationship between the average full trace length and the average diameter of the outcrop surface when the fracture diameter obeys the negative exponential distribution. Wu [27] suggested that the average full trace length of the outcrop intersection and the fracture diameter is the average chord length of the circular fracture diameter. Based on this, he proposed a new formula for estimating the diameter of the fracture diameter using the full trace length of the outcrop. Zhang and Einstein [28] deduced the calculation formula of the average full trace length of the outcrop surface and estimated the average diameter using the circular statistical window method. Huang [29] estimated the full trace length of the outcrop surface based on the half trace length intersected with the survey line and then estimated the average diameter through the average full trace length of the outcrop surface, and corrected the error caused by the truncation value in the process. Hekmatnejad et al. [30] estimated the fracture diameter using the numerical integration method by comparing measured and calculated values with full track length as calibration parameters. In addition, Tonon and Chen [31] derived the average diameter and fracture diameter distribution for the common probability distribution form of the full trace length of the outcrop surface. Zhang and Einstein [32] proposed the polynomial form of the probability density function for the track length distribution under the infinite measuring window and derived the analytical solution of the corresponding probability density function for the diameter distribution. Based on the fact that the disk center is uniformly distributed in the three-dimensional space, the spatial model of the intersection of the fracture and the measuring line, the spatial model of the intersection of the fracture and the rectangular window, and the spatial model of the intersection of the fracture and the rectangular box with the rectangular window as a plane are established by applying the principle of probability statistics. Finally, the average value of the

fracture diameter and the expected value of the fracture are obtained.

*2.1. The Intersection Model of the Fractures and the Scanline in Space.* The method in this paper assumes that a fracture in space is a thin disk. Consider that  $\theta$  is the dip direction of the fracture,  $\alpha$  is the dip angle of the fracture,  $D$  is the diameter of the fracture, and  $\vec{n}$  is the normal vector of the disk. In this case, there is a scanline whose length is random. Let  $l$  be the length,  $\vec{m}$  be the direction vector, and  $\alpha_{mn}$  ( $\alpha_{mn} \in [0,90]$ ) be the intersecting angle of the scanline and the normal direction of fracture. If the fracture intersects with the given scanline, then the center point of the fracture must be in the oblique cylinder as shown in Figure 2. Let  $V_l$  be the volume of the oblique cylinder, then  $V_l$  can be obtained from equation (1) as follows:

$$V_l = \frac{1}{4} \pi D^2 l \cos \alpha_{mn}. \quad (1)$$

Assume that the center of the fracture is in the three-dimensional space, the disk center's is uniformly distributed, and the volume density of the center distribution is  $\lambda$ . Let  $f(D)$  be the distribution function of the disk diameter and  $f(\theta, \alpha)$  be the distribution function of fracture dip direction and angle. Furthermore, assume that the orientation and size of the fracture are independent of each other. Let  $N_{L1}$  be the expected value of the number of fractures obtained from arbitrary disk diameter and arbitrary fracture orientation intersecting with the given scanline.  $N_{L1}$  can be expressed as equation (2).

$$\begin{aligned} N_{L1} &= \lambda \int_0^\infty \int_{\alpha_l}^{\alpha_\alpha} \int_{\theta_l}^{\theta_\alpha} V_l f(D) f(\theta, \alpha) d\theta d\alpha dD \\ &= \lambda \int_0^\infty \int_{\alpha_l}^{\alpha_\alpha} \int_{\theta_l}^{\theta_\alpha} \frac{1}{4} (\pi D^2 l \cos \alpha_{mn}) f(D) f(\theta, \alpha) d\theta d\alpha dD. \end{aligned} \quad (2)$$

Based on the properties of the probability density function, the following formulas can be obtained. Because  $\int_0^\infty f(D) dD = 1$ ,  $\int_0^{90} g(\alpha_{mn}) d\alpha_{mn} = 1$ , and  $\int_{\alpha_l}^{\alpha_\alpha} \int_{\theta_l}^{\theta_\alpha} \cos \alpha_{mn} d\theta d\alpha = E(\cos \alpha_{mn})$ , then put the above three formulas into equation (2),  $N_{L1}$  can be obtained from equation (3).

$$N_{L1} = \frac{1}{4} \lambda \pi l E(D^2) E(\cos \alpha_{mn}). \quad (3)$$

However, the fracture center is not strictly uniformly distributed in the actual rock engineering, and the measured  $N_{L1}$  by setting one scanline has certain contingency and instability. The single scanline method has an inevitable occurrence of sampling deviation. Hence, the

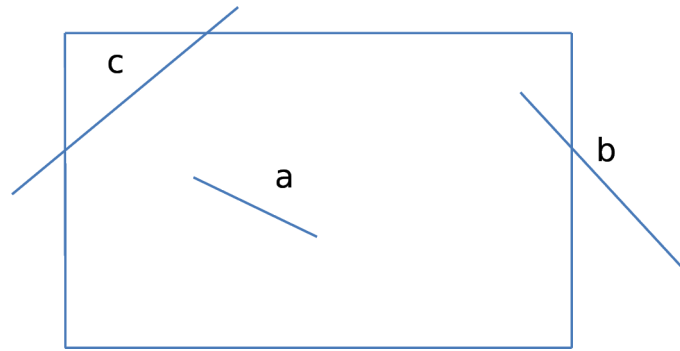


FIGURE 1: The three types of intersecting states between trace length and sampling window can be expressed as  $a$ ,  $b$ , and  $c$ .

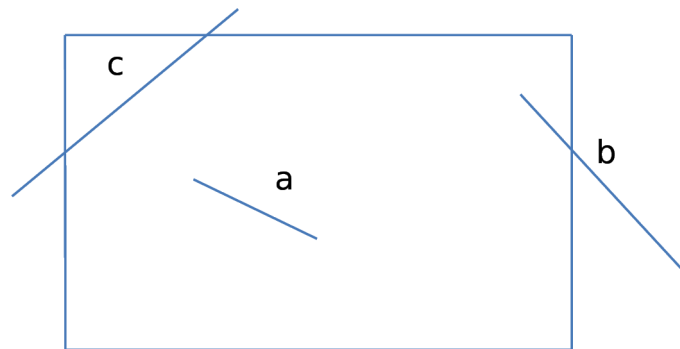


FIGURE 2: Schematic diagram of the center area of the intersection of fracture and scanline.

single scanline preferentially intersects the fracture with a large intersection angle. At the same time, the layout of the single scanline method selects the place where the fracture intersects the most. However, this cannot truly reflect the fracture distribution and the corresponding trace length. The scanlines method mentioned in this paper is similar to the gridding of the rectangular window and can fully reflect the overall distribution characteristics of the fracture in the window. Therefore, reasonably arranging the scanlines is very important, but it is a very complex task. The scanline layout method involves determining its number, length, direction, and position. For different window trace distributions, the method of line layout should vary. The basic principle of scanlines arrangement is that the scanlines arranged should reflect the distribution of all traces in the window as accurately as possible. Generally, when the window is covered with uniform and equidistant orthogonal grids, the grid lines are taken as scanlines, so that the overall distribution of traces in the window on the two-dimensional plane can be reasonably reflected. The reasonable number of measuring lines or the density of the measuring line arrangement is related to the number of trace lines in the window and the exposure form, as shown in Figure 3. In this study, it is suggested that the total number of orthogonal scanlines in the sampling window should be  $N_c = 2N_2 + N_1$ , where  $N_2$  is the number of traces whose both ends are observable, and  $N_1$  is the number of traces whose only one end is observable. This value is a suggested value because the number of trace endpoints in the window surface can reflect the denseness of the trace's

midpoint in the window. Therefore, selecting the number of measured lines can effectively reflect the overall distribution of the window traces.

Assume that the average value of intersecting traces measured by multiple lines with the same length parallel to the  $w$  side is  $N_{Lw}$ , and the average value of intersecting traces measured by multiple lines with the same length parallel to the  $h$  side is  $N_{Lh}$ , then  $N_{Lw}$  and  $N_{Lh}$  can be obtained from equations (4) and (5).

$$N_{Lw} = \frac{\sum_{i=1}^{N_c} N_{Lwi}}{N_c} = \frac{1}{4} \lambda \pi w E(D^2) E(\cos \alpha_{wn}), \quad (4)$$

$$N_{Lh} = \frac{\sum_{i=1}^{N_c} N_{Lhi}}{N_c} = \frac{1}{4} \lambda \pi h E(D^2) E(\cos \alpha_{hn}). \quad (5)$$

Let  $N_L$  be the average value of intersecting traces measured by multiple lines in rectangular sampling, then  $N_L$  can be obtained from equation (6).

$$N_L = N_{Lw} + N_{Lh} = \frac{1}{4} \lambda \pi E(D^2) [w E(\cos \alpha_{wn}) + h E(\cos \alpha_{hn})]. \quad (6)$$

**2.2. The Intersection Model of the Fractures and the Rectangular Window in Space.** In a rectangular window,  $\alpha_{wn}$  is the intersection angle of the disk normal direction and  $w$  side direction,  $\alpha_{hn}$  is the intersection angle of the

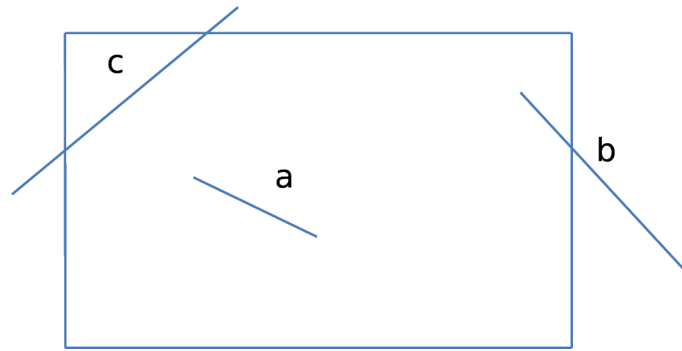


FIGURE 3: Schematic diagram of the single line method (a) and the scanlines method (b).

disk normal direction and  $h$  side direction, and  $\alpha_{bn}$  is the intersection angle of the disk and the rectangular window in normal direction. If the fracture is intersected with the rectangular window, the center point of the fracture must be in the finite region as shown in Figure 4. This region consists of three parts: (1) the top and bottom are the semioblique columns with the  $w$  side as the generatrix, (2) the right and left are the semioblique columns with the  $b$  side as the generatrix, and (3) the middle area is an oblique cube. Then, the volume of this region ( $V_p$ ) can be derived from equation (7) as

$$V_p = \frac{1}{4}\pi D^2(w\cos\alpha_{wn} + h\cos\alpha_{hn}) + whD\sin\alpha_{bn}. \quad (7)$$

In order to make the expression not show the probability density function of  $\alpha_{wn}$ ,  $\alpha_{hn}$ , and  $\alpha_{bn}$ , this paper adopts the probability density function of fracture orientation  $f(\theta, \alpha)$  instead of integrating so that the integration will not cause a correlation problem.

Assume that the disk center is uniformly distributed in the three-dimensional space,  $\lambda$  is the volume density of the center distribution,  $f(d)$  is the distribution function of the disk diameter size,  $f(\theta, \alpha)$  is the distribution function of the fracture dip direction and angle and the orientation of fractures independent of fracture size. Accordingly, the expected value of the fracture number  $N_p$  is obtained from the arbitrary disk diameter, and the orientation of the fracture intersecting with the given scanline can be expressed as equation (8).

$$\begin{aligned} N_p &= \lambda \int_0^\infty \int_{\alpha_l}^{\alpha_u} \int_{\theta_l}^{\theta_u} V_L f(D) f(\theta, \alpha) d\theta d\alpha dD \\ &= \lambda \int_0^\infty \int_{\alpha_l}^{\alpha_u} \int_{\theta_l}^{\theta_u} \left[ \frac{1}{4}\pi D^2(w\cos\alpha_{wn} + h\cos\alpha_{hn}) \right. \\ &\quad \left. + whD\sin\alpha_{bn} \right] f(D) f(\theta, \alpha) d\theta d\alpha dD. \end{aligned} \quad (8)$$

Because

$$\begin{aligned} \int_0^\infty f(D) dD &= 1, \int_0^\infty D f(D) dD = E(D), \int_0^\infty D^2 f(D) dD \\ &= E(D^2), \\ \int_{\alpha_l}^{\alpha_u} \int_{\theta_l}^{\theta_u} d\theta d\alpha &= 1, \int_{\alpha_l}^{\alpha_u} \int_{\theta_l}^{\theta_u} \cos\alpha_{wn} d\theta d\alpha E(\cos\alpha_{wn}) \end{aligned}$$

$$\begin{aligned} \int_{\alpha_l}^{\alpha_u} \int_{\theta_l}^{\theta_u} \cos\alpha_{hn} d\theta d\alpha &= E(\cos\alpha_{hn}) \quad \text{and} \\ \int_{\alpha_l}^{\alpha_u} \int_{\theta_l}^{\theta_u} \cos\alpha_{wn} d\theta d\alpha &= E(\sin\alpha_{bn}) \end{aligned}$$

Then, the above equation (8) can be simplified to equation (9)

$$\begin{aligned} N_p &= \frac{1}{4}\lambda\pi E(D^2)[wE(\cos\alpha_{wn}) + hE(\cos\alpha_{hn})] \\ &\quad + \lambda wh E(D) E(\sin\alpha_{bn}). \end{aligned} \quad (9)$$

The result shows that using the fracture orientation data as an integral variable is more reasonable.

2.3. *The Intersection Model of the Fractures and the Cuboid With the Rectangle Sampling Window in Space.* Assume that there is a rectangular box with the rectangle sampling window,  $w$ ,  $b$ , and  $h$  are the length, width, and height of the rectangular box, respectively, as shown in Figure 5. If the fracture whose diameter and normal vector are  $D$  and  $\vec{n}$  intersects with the rectangular box, the fracture center must be located in the volume  $V_v$  enclosed by the fracture center that exactly meets the surface of the cuboid. The volume  $V_v$  consists of three parts: (1) the volume of the oblique cylinder whose genera traces are  $w$ ,  $h$ , and  $b$ , (2) the rhombic volume with front, side, and top surfaces, and (3) the volume of the cuboid itself. Then,  $V_v$  can be derived from equation (10).

$$\begin{aligned} V_v &= \frac{1}{4}\pi D^2(w\cos\alpha_{wn} + h\cos\alpha_{hn} + b\cos\alpha_{bn}) \\ &\quad + (whD\sin\alpha_{bn} + wbD\sin\alpha_{hn} + hbD\sin\alpha_{wn}) + whb. \end{aligned} \quad (10)$$

In this paper, the integral range of the fracture size ranges from 0 to infinity; hence, the volume formed by the center point of the fracture intersecting with the cubic box is irrelevant to fracture size, except that when the diameter of the structural surface is small, according to equation (10), the volume  $V_v$  is close to  $whb$ . Therefore, equation (10) is reasonable.

Assume that the disk center is uniformly distributed in the three-dimensional space, and  $\lambda$  is the volume density of the center distribution. Similarly, the expected value of the fracture number  $N_v$  is obtained from the arbitrary disk

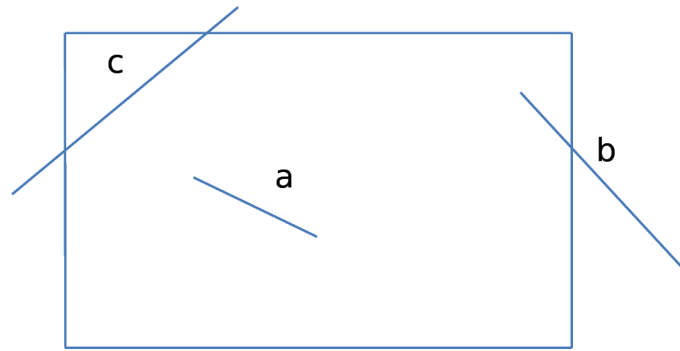


FIGURE 4: It is the schematic of the region of the fracture center point when the fracture is intersected with a rectangular window.

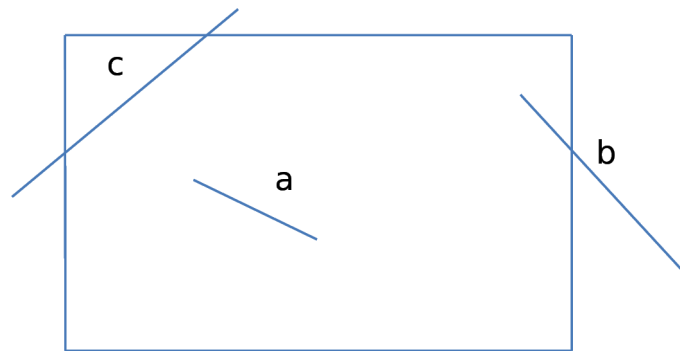


FIGURE 5: Schematic of the fracture center point region when the fracture is intersected with a rectangular box.

diameter, and the orientation of the fracture intersect with the given rectangular window can be expressed as equation (11).

$$N_v = \frac{1}{4} \lambda \pi E(D^2) [wE(\cos \alpha_{wn}) + hE(\cos \alpha_{hn}) + bE(\cos \alpha_{bn})] + \lambda E(D) [whE(\sin \alpha_{bn}) + wbE(\sin \alpha_{hn}) + hbE(\sin \alpha_{wn})] + \lambda whb. \quad (11)$$

**2.4. Model Solving When  $N_v$  Is Known.** Assume that in a certain space, the disk center is uniformly distributed, and  $\lambda$  is the volume density of the center distribution. If the number of fractures that intersect with a given rectangular box ( $N_v$ ), the number of fractures that intersect with a given rectangular sampling window ( $N_p$ ) and the number of fractures that intersect with a given line ( $N_l$ ) are all known, then, the following equation (12) can be obtained using equations (6), (9), and (11).

$$\lambda = \frac{4N_l}{C_0 E(D^2)} = \frac{4N_p}{A_1 E(D^2) + 4A_2 E(D)} = \frac{4N_v}{B_1 E(D^2) + B_2 E(D) + 4whb}. \quad (12)$$

In equation (12),

$$A_1 = \pi [wE(\cos \alpha_{wn}) + hE(\cos \alpha_{hn})],$$

$$A_2 = whE(\sin \alpha_{bn}),$$

$$B_1 = \pi [wE(\cos \alpha_{wn}) + hE(\cos \alpha_{hn}) + bE(\cos \alpha_{bn})],$$

$$B_2 = whE(\sin \alpha_{bn}) + wbE(\sin \alpha_{hn}) + hbE(\sin \alpha_{wn}),$$

$$C_0 = \pi wE(\cos \alpha_{wn}) + \pi hE(\cos \alpha_{hn}),$$

Equations (13) and (14) can be obtained from equation (12) after derivation and arrangement.

$$E(D^2) = \frac{4whbN_l A_2}{N_v A_2 C_0 - N_l A_2 B_1 - N_p B_2 C_0 + N_l A_1 B_2}, \quad (13)$$

$$E(D) = \frac{whb(N_p C_0 - N_l A_1)}{N_v A_2 C_0 - N_l A_2 B_1 - N_p B_2 C_0 + N_l A_1 B_2}. \quad (14)$$

The diameter of the fractured disk can be obtained from equation (14) when  $N_v$  is known.

**2.5. Model Solving When  $N_v$  Is Unknown.** Indeed, it is very difficult to obtain  $N_v$  in practical rock engineering. Therefore it is necessary to estimate the value of  $N_v$  accurately and effectively to make the average diameter estimation method proposed in this paper applicable to practical rock engineering. In practical rock engineering, the fracture properties intersected with rectangular window is easily understood. Figure 6 is the top view of the center area of the intersection of cuboid box and fractures. Because

the fracture center is assumed to be evenly distributed in three-dimensional space, therefore, when the rectangular plane is parallel to a rectangular window in a cuboid, the expected value of the intersecting fracture of the rectangular plane is the same as the number of trace lines seen in the window. For the fracture whose average diameter is  $E(D)$  and the angle expectation in the direction of  $b$  is  $E(\sin \alpha_{bn})$ , when the fracture exactly intersects with the two rectangular planes in the direction of  $b$ , then the distance between the two rectangular plane is  $E(D)E(\sin \alpha_{bn})$ . The center volume ( $V_v$ ) of the fracture intersected with the cuboid box can be equivalent to the center volume of fracture planes intersecting with the rectangular window, where  $n_b = \frac{b}{E(D)E(\sin \alpha_{bn})} + 1$ . Nevertheless, such equivalence does not consider the void volume caused by replacing the volume of the trapezoid with the oblique cylinder volume in the direction of the  $w$ -side of the top and bottom sides, the  $h$ -side of the left and right sides, and the  $b$ -side of the front and behind sides. The void in Figure 6 is the projection of the gap in the direction of the  $h$ -side of the left and right sides on the horizontal plane. The number of fracture centers in the gap between the  $w$  and  $h$  edges can be estimated from  $N_{lw}$  and  $N_{lh}$  measured on the window surface. Accordingly, the number of fracture centers in the direction of  $w$  in the top and bottom of the gap is  $n_w$ , where  $n_w = \frac{b}{E(D)E(\sin \alpha_{bn})} \frac{4 - \pi}{2\pi} E(\cos \alpha_{wn}) N_{lw}$ . The number of fracture centers in the direction of  $h$  on right and left of the gap is  $n_h$ , where

Assume that the number of fracture centers in the  $b$ -side gap is  $N_b$ . Hence,  $N_v$  can be derived from equation (15):

$$N_v = \frac{b + E(D)E(\sin \alpha_{bn})}{E(D)E(\sin \alpha_{bn})} N_p + \frac{b}{E(D)E(\sin \alpha_{bn})} \frac{4 - \pi}{2\pi} [2E(\cos \alpha_{wn})N_{lw} + 2E(\cos \alpha_{hn})N_{lh}] + N_b. \quad (15)$$

In this study, equation (16) is recommended as the estimation equation of  $N_v$  value because the  $N_b$  value on the  $b$ -side cannot be obtained from in the window plane. Thus equation (15) can be simplified to derive equation (16) as follows:

$$N_v \approx \frac{b + E(D)E(\sin \alpha_{bn})}{E(D)E(\sin \alpha_{bn})} N_p + \frac{b}{E(D)E(\sin \alpha_{bn})} \frac{4 - \pi}{2\pi} (2N_{lw} + 2N_{lh}). \quad (16)$$

Because  $N_l = N_{lw} + N_{lh}$ , equation (16) can be simplified as follows:

$$N_v \approx \frac{b + E(D)E(\sin \alpha_{bn})}{E(D)E(\sin \alpha_{bn})} N_p + \frac{b}{E(D)E(\sin \alpha_{bn})} \frac{4 - \pi}{\pi} N_l. \quad (17)$$

In general, equations (12) and (17) can be used to obtain the estimated formula for the average diameter of the fracture when  $N_v$  is unknown as follows:

$$E(D^2) = \frac{(4\pi A_2 C_0 b N_p + 16 A_2 C_0 b N_l - 4\pi A_2 C_0 b N_l - 4\pi E(\sin \alpha_{bn}) C_0 w h b N_p + 4\pi E(\sin \alpha_{bn}) A_1 w h b N_l) A_2 N_l}{\pi E(\sin \alpha_{bn}) (C_0 N_p - A_1 N_l) (A_2 B_1 N_l + B_2 C_0 N_p - A_1 B_2 N_l - A_2 C_0 N_p)}. \quad (18)$$

$$E(D) = \frac{\pi A_2 C_0 b N_p + 4 A_2 C_0 b N_l - \pi A_2 C_0 b N_l - \pi E(\sin \alpha_{bn}) C_0 w h b N_p + \pi E(\sin \alpha_{bn}) A_1 w h b N_l}{\pi E(\sin \alpha_{bn}) (A_2 B_1 N_l + B_2 C_0 N_p - A_1 B_2 N_l - A_2 C_0 N_p)}. \quad (19)$$

Equations (18) and (19) are the fracture diameter estimation formulas for the unknown  $N_v$ . In order to fully reflect the distribution of the fractures in space by the fractures in the rectangular box, the value of  $b$  in equations (18) and (19) should be taken as the length of the larger rectangular window's side.

### 3. Application of Mathematical Model

**3.1. Application to a Simulated Case.** Randomly generate 20,000 fractures in a  $100 \times 100 \times 100$  m cube, with an average dip direction of  $200^\circ$  and an average dip angle of  $55^\circ$ . A small cube of  $40 \times 40 \times 40$  m is placed at the center of the cube to avoid the edge affect. Figure 7 indicates the fracture surface intersecting with this small cube, where the number of fracture surfaces is  $N_v = 780$ , and one cube surface is considered  $abcd$ . The trace of the visible window plane is depicted in Figure 8, where  $N_p = 110$ ,  $R_0 = 0.0091$ ,  $R_1 = 0.3$ ,  $R_2 = 0.6909$ , and  $N_c = 2N_2 + N_1 = 185$ . Therefore, by arranging 185 sets of orthogonal survey lines within the rectangular window, the estimated result of the fracture surface diameter of the new method can be obtained. The real fracture diameter situation, the new method's calculation result, and the calculation result of the Kulatilake trace length integral fracture diameter estimation approach are compared in Table 1.

The data comparison in Table 1 indicates that the new method is more precise in estimating the mean value of the structural surface diameter, the mean square diameter, and the  $N_v$  value. Therefore, the proposed approach for estimating the average diameter of the fracture in this paper is accurate and effective.

**3.2. Application to Practical Rock Engineering.** The new fracture diameter probability estimation method is applied to estimate the average fracture diameter of a dominant group in the Songta Hydropower Station. The site survey of an adit of Songta Hydropower Station is shown in Figure 9. The dominant group has a total of 58 structural surfaces, with an average inclination of  $351.6^\circ$  and  $82.75^\circ$ . The window for statistical traces in the flat cave is vertical at

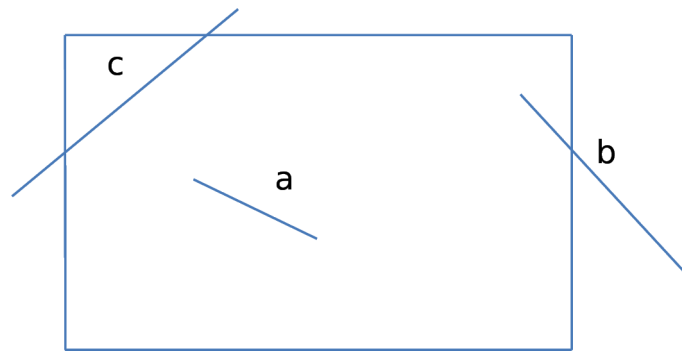


FIGURE 6: Top view of the central area of the intersecting fracture of the box.

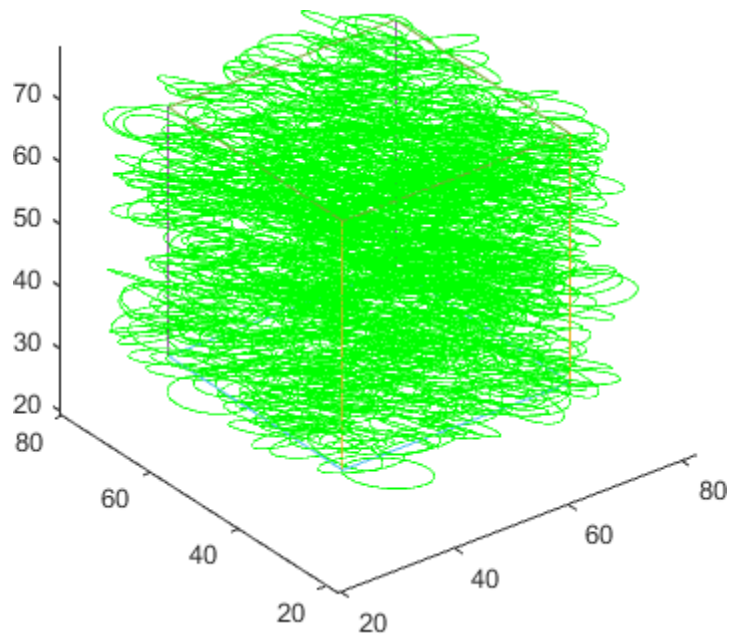


FIGURE 7: Distribution of fractures intersecting with a  $40 \times 40 \times 40$  m cube.

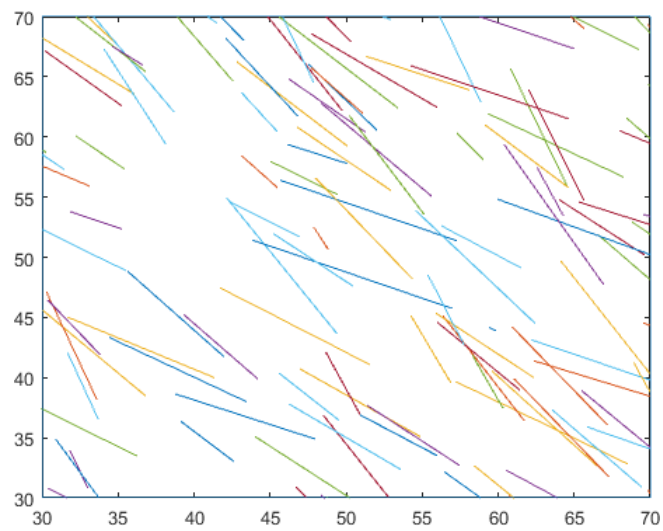


FIGURE 8: Representation of window plane trace distribution.



TABLE 1: The calculation results of the new method, the comparison between the Kulatilake trace length integration method, and the actual value  $m^2$ .

		Average diameter ( $m$ )	The square of the average diameter ( $m^2$ )	$N_v$
Truth value		5.0104	33.3252	780
Scanlines method	Calculation results	5.2841	30.3138	797
	Error rate (%)	5.18 %	9.93 %	2.1 %
Kulatilake method	Calculation results	4.3870	20.0253	-
	Error rate (%)	14.21 %	66.42 %	-

54 m long and 2 m high and runs north to south. Figure 10 illustrates the measured window trace.

Figure 8 reveals that  $R_0 = 0.0517$ ,  $R_1 = 0.4138$ , and  $R_2 = 0.5345$  and the total number of survey lines arranged in the window  $N_c = 2N_2 + N_1 = 86$ ; the average trace length of the observation is 1.1899 m, and the average trace length of multiple traces is applied. The average value of the trace length calculated by the estimation method is 2.5541 m. Using Kulatilake's trace length integration method, the average diameter of the structural surface is 2.66 m, and the average diameter squared is 7.92  $m^2$ . The average diameter of the fracture is 2.9662 m, and the average square of the diameter is 13.2462  $m^2$  utilizing the new approach.

**3.3. Estimation of the Probability Density Function of Disk Diameter.** The expected value of disk diameter and the square of disk diameter can be obtained from equations (18) and (19). In addition, the probability density function of the two-dimensional full trace can be determined by the estimation method of the mean trace length presented by Zhang [17]. The above conditions are unavailable when the traditional Kulatilake approach estimates the disk diameter probability density function. Based on these conditions, this paper assumes that the form of the probability density function of the disk diameter and the two-dimensional full trace is identical and then presents a new disk diameter probability density estimation method.

Since the expected value of disk diameter and the square of disk diameter are known, equation (20) can be described according to the variance definition of the probability density function.

$$D(X) = E(X^2) - [E(X)]^2, \quad (20)$$

where  $D(X)$  is the variance of fracture disk diameter,  $E(X^2)$  is the expected value of fracture disk diameter, and  $[E(X)]^2$  is the expected value of the square of disk diameter.

Then based on the known form of the probability density function of the disk diameter, the expected value, and variance of the diameter, the parameters of the disk probability density function can be precisely estimated.

In order to verify the above theory, 20,000 disks are randomly generated in a three-dimensional space of  $100 \times 100 \times 100$  m, and their diameters are subject to a lognormal distribution. The average diameter is 10 m, and the variance is 10  $m^2$ . The two parameters of the lognormal distribution are  $a$  and  $b$ . Parameter  $a$  is 2.2549 and  $b$  is 0.0953. The

study area consists of a  $40 \times 40 \times 40$  m cubic in the center of the area to avoid the edge effect. One face of the cube is considered a visible window, and Figure 11 depicts the window trace distribution.

The window contains 192 traces, in which  $R_0 = 0.0313$ ,  $R_1 = 0.4844$ , and  $R_2 = 0.4844$ , the actual trace length is 8.3613 m, the result of applying the Kulatilake trace length estimation method is 8.1712 m, and the finding of using the scanlines approach is 8.1947 m; the scanlines method yields a more accurate result. By employing the scanlines method to estimate the trace length probability density function, the actual, estimated, and observed trace frequency bar charts are depicted in Figures 12–14. The actual, estimated, and observed trace length probability density curve can be fitted based on the value of trace length probability density in different conditions as shown in Figure 15. Table 2 lists the actual, estimated, and observed trace length probability density curve parameters.

Figure 15 and Table 2 indicate that the estimated and actual trace length curves are close to each other, regardless of the curve shape and the function parameters, and the fitting function is a lognormal distribution function.

The scanlines disk diameter estimation method produces an average disk diameter of 9.4 m and a diameter square of 98.3  $m^2$ . Based on equation (20), the diameter variance can be obtained as 9.94  $m^2$ . On the assumption that the disk diameter and the trace length of fracture have the same type of probability density function, the disk diameter of the fracture also obeys the lognormal distribution and has the property of lognormal distribution, as demonstrated by equations (21) and (22).

$$a = \ln(E(X)) - \frac{1}{2} \ln \left( 1 + \frac{D(X)}{E(X)^2} \right), \quad (21)$$

$$b = \ln \left( 1 + \frac{D(X)}{E(X)^2} \right), \quad (22)$$

where  $a$  and  $b$  are the parameters of the lognormal distribution function,  $E(X)$  is the expected value of disk diameter, the value of  $E(X)$  is 9.4 m,  $D(X)$  is the variance expected value of disk diameter, and the value of  $D(X)$  is 9.94  $m^2$ .

Therefore, the equations (21) and (22) can be utilized to determine the parameter values of the lognormal

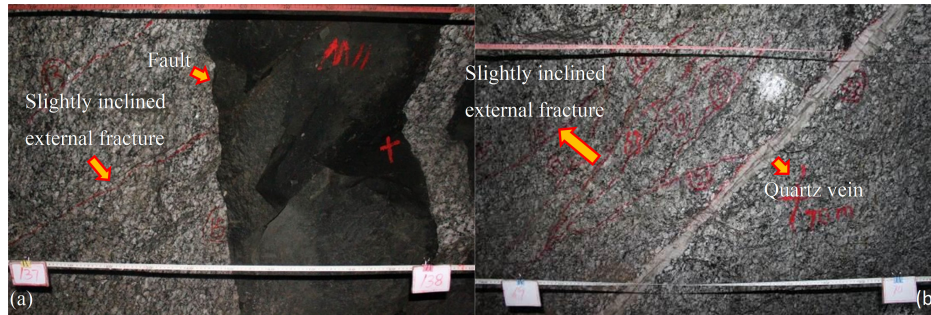


FIGURE 9: Site survey map of an adit of Songta Hydropower Station.

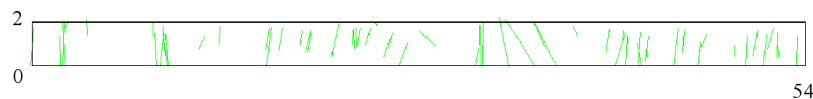


FIGURE 10: The measured window trace.

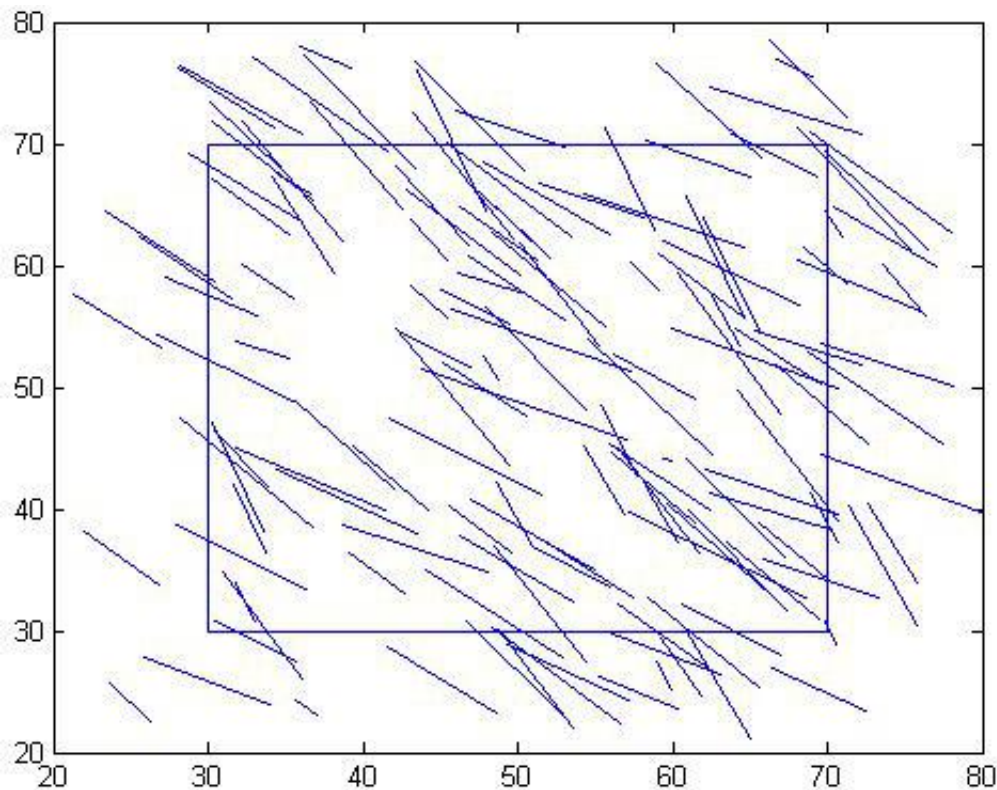


FIGURE 11: The trace distribution of visible window.

distribution governed by the disk diameter. In the simulation, the parameter  $a$  is set to 2.2549, while the parameter  $a$  is computed to be 2.1874. The parameter  $b$  set during simulation is 0.0953, while the parameter  $b$  estimated through calculation is 0.1066. It can be seen that the estimated parameters are more consistent with the parameters set during the simulation.

Using the proposed method in this paper to estimate the fracture disk diameter is applicable not only in the case that the probability density function of the observed trace length of fracture in the example of this paper obeys the

lognormal distribution but also in the situation that the probability density function of the observed trace length of fracture follows other probability density functions [33]. This is due to the paper's assumption that the probability density function of the fracture disk diameter and trace length are identical. Therefore, as long as the probability density function of the observed trace length of fracture is obtained, then using equations (18) and (19), the expected value of disk diameter and the square of disk diameter can be obtained, and the variance of the disk diameter can be obtained by substituting equation (20). Finally, based on

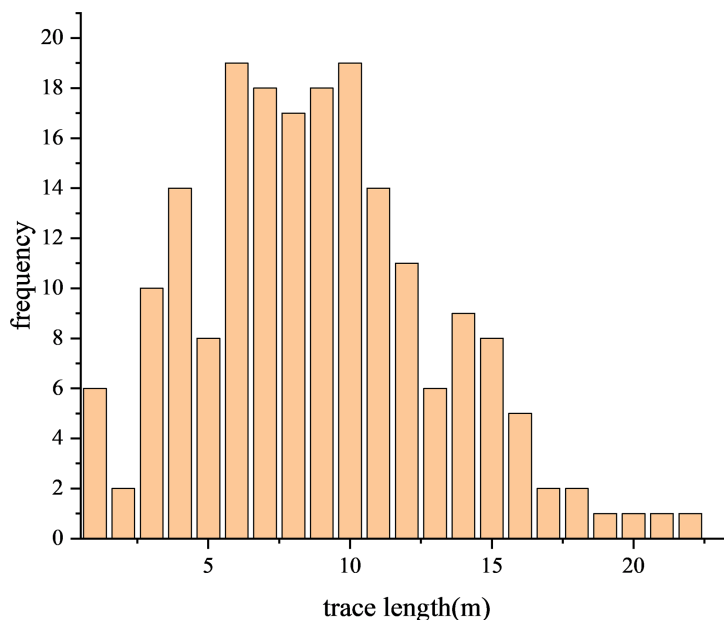


FIGURE 12: The frequency histogram of actual track length.

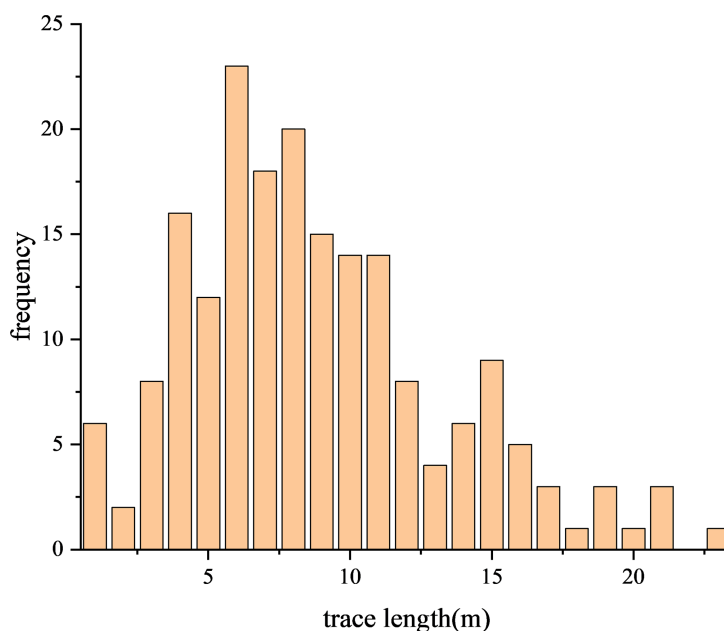


FIGURE 13: The frequency histogram of estimated track length.

the parameter calculation formulas corresponding to the various functions in Table 3, it is possible to determine the parameters of the probability density function of the fracture disk that corresponds to various density functions. The specific calculation process is illustrated in Figure 16.

#### 4. Conclusion

This paper proposes a new method for estimating the disk diameter of the fracture. Based on the fact that the center of the disk is uniformly distributed in the three-dimensional

space, the space intersection model of arbitrary fracture and scanline, rectangular window and a rectangular box with a rectangular window is derived using the principle of probability statistics. The expected value of disk diameter and the square of disk diameter can be calculated utilizing equations (18) and (19). This paper presents a new disk diameter probability density estimation method. Several conclusions can be drawn from this paper:

- (1) The model's solution determines the expected value of the fracture diameter and its square. However, the

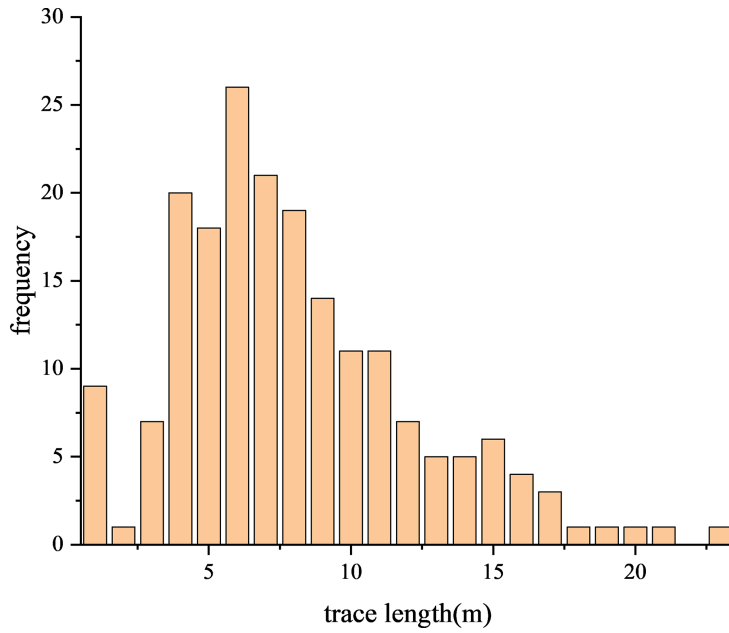


FIGURE 14: The frequency histogram of observed track length.

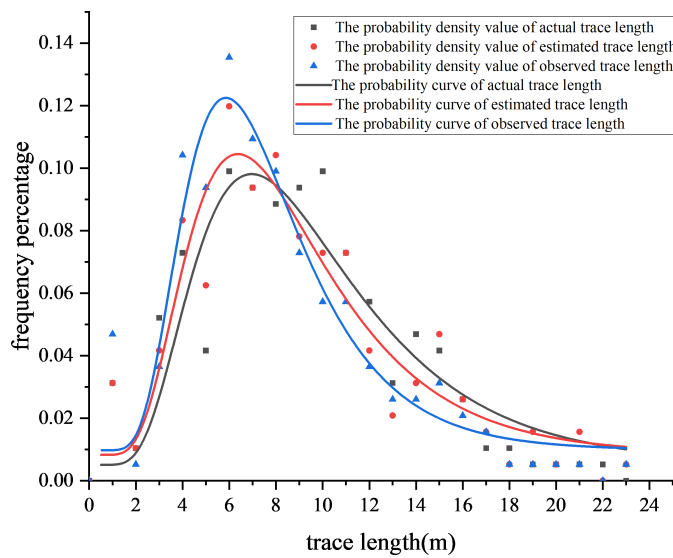


FIGURE 15: The probability density curves of actual, estimated, and observed trace length.

TABLE 2: Statistical table of the actual, estimated, and observed trace length probability density curve parameters.

Method	The actual trace length fitting curve	The estimated trace length fitting curve	The observed trace length fitting curve
Parameter <i>a</i>	2.058	2.058	1.956
Parameter <i>b</i>	0.3145	0.3192	0.2931

number of fractures intersecting the box ( $Nv$ ) is used in the solution process. If the actual project can effectively obtain the  $Nv$  value, equations (18) and (19) can be utilized to solve the problem.

- (2) If the  $Nv$  value is difficult to obtain in the actual project, an effective and reasonable estimate of the  $Nv$  value is required. In this paper, the estimation

formula of  $Nv$  value is deduced using window intersection traces. Furthermore, under the condition that  $Nv$  can not be obtained, a reasonable estimation of the average diameter of the fracture can be established, which extends the application range of the proposed method.

TABLE 3: Parameters calculation table for different density functions.

Density function	Expression	Parameter calculation formula	
Normal distribution	$f(x) = \frac{1}{\sqrt{2\pi}\sigma} e^{-\frac{(x-\mu)^2}{2\sigma^2}}$	$\mu = E(X)$	$\sigma^2 = D(X)$
Lognormal distribution	$f(x) = \frac{1}{x\sqrt{2\pi}b} e^{-\frac{\ln(x-a)^2}{2b}}$	①	$b = \ln\left(1 + \frac{D(X)}{E^2(X)}\right)$
Gamma distribution	$f(x) = \frac{x^{(\alpha-1)}\lambda^\alpha e^{-\lambda x}}{\Gamma(\alpha)}$	$\alpha = \frac{E^2(X)}{D(X)}$	$\lambda = \frac{E(X)}{D(X)}$
Index distribution	$f(x) = \lambda e^{-\lambda x}$	$\lambda = \frac{1}{E(X)}$	—
Rayleigh distribution	$f(x) = \frac{x}{\sigma^2} e^{-\frac{x^2}{2\sigma^2}}$	$\sigma = E(X)\sqrt{\frac{2}{\pi}}$	—
Evenly distribution	$f(x) = \frac{1}{b-a}$	②	③
Beta distribution	$f(x) = \frac{x^{(\alpha-1)}(1-x)^{(\beta-1)}}{B(\alpha, \beta)}$	④	⑤

①  $a = \ln(E(X)) - \frac{1}{2} \ln\left(1 + \frac{D(X)}{E(X)^2}\right)$ , ②  $a = E(X) - \sqrt{3D(X)}$ , ③  $b = E(X) + \sqrt{3D(X)}$ , ④  $\alpha = \frac{E^2(X)(1-E(X))}{D(X)} - E(X)$ , and ⑤  $\beta = \frac{E^2(X)(1-E(X))^2}{E(X)D(X)} + E(X) - 1$ .

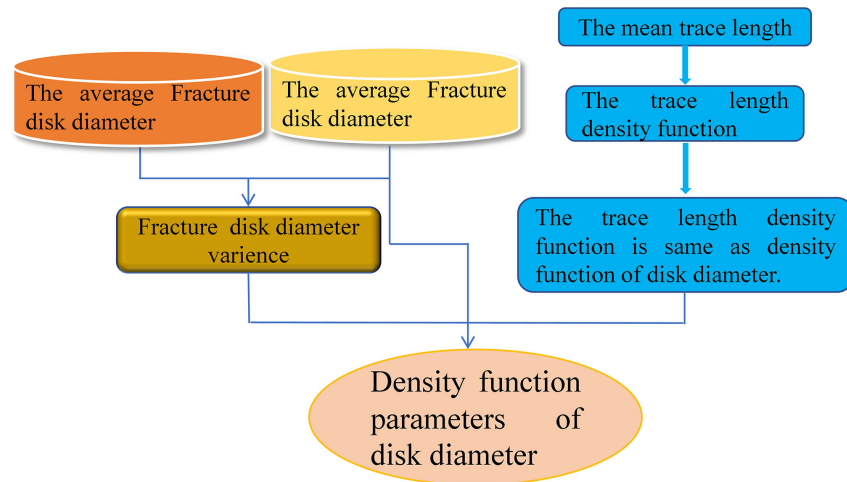


FIGURE 16: The technical flow chart of finding the mean value of disk diameter and density function.

- (3) Randomly generated fracture data and engineering examples are applied to test the proposed approach and compared with the traditional Kulatilake track length integral evaluation method. The results showed that this technique reasonably estimates the average fracture diameter.
- (4) The disk probability density function parameters are precisely estimated based on the known probability density function of the disk diameter, the expected diameter, and the diameter variance.

The traditional Kulatilake uses the concepts of conditional probability and geometric probability to establish the relationship between the probability density of trace length and the probability density of fracture diameter. The given numerical solution method can obtain fracture diameter distribution through the probability density function with different trace lengths. Therefore, it is very important to obtain accurate trace length data. The traditional Kulatilake uses the single-line method to calculate the trace length. The single-line method inevitably has the occurrence sampling deviation, that is, the survey line preferentially intersects the fracture with a relatively large intersection angle

with it. Meanwhile, in the single-line method, because the probability of intersection between the survey line and the disk decreases with the reduction of the disk diameter, most of the small fracture diameter do not cut the sampling window. Thus, the average trace length is only those fractures surfaces with large diameter and intersecting with the sampling surface. Therefore, the error of the fracture diameter obtained is large. The multiline method can obtain a more comprehensive intersection of the line and the trace length, so it can obtain a more accurate trace length and fracture diameter. The method proposed in this paper can well estimate the mean value of fracture diameter and is a generalized method for estimating the average fracture diameter in actual rock mass engineering.

In summary, the proposed method in this research uses the principle of probability statistics and can estimate the average fracture diameter with reasonable accuracy. It is a generalized approach for predicting the mean fracture disk diameter.

When the number of fractures intersecting the rectangular box  $N_v$  is unknown, this research approximates this statistic in the theoretical derivation of the proposed method in this research for calculating the fracture disk diameter. In the future, more effective and accurate methods can be used to calculate the value of  $N_v$ , which can also be obtained through field investigation.

## Data Availability Statement

The data can be available by contacting the corresponding author or the first author.

## Conflicts of Interest

The authors declare no conflict of interest.

## Acknowledgments

This paper is sponsored by the National Natural Science Foundation of China (Grant No. 41941017 and U1702241). Prof. Jianping Chen is the principal director of the fund.

## References

- [1] J. P. Chen, S. F. Xiao, and Q. Wang, *Computer Simulation Principle of 3D Random Discontinuities Network*, Northeast Normal University Press, Changchun, Jilin, 1995.
- [2] M. Gao, W. Jin, R. Zhang, J. Xie, B. Yu, and H. Duan, "Fracture size estimation using data from multiple Boreholes," *International Journal of Rock Mechanics and Mining Sciences*, vol. 86, July, pp. 29–41, 2016.
- [3] A. Robertson, "The interpretation of geological factors for use in slope theory," *Planning Open Pit Mines*, 55–71, 1970.
- [4] V. M. Narendran and M. P. Cleary, "Elastostatic interaction of multiple arbitrarily shaped cracks in plane inhomogeneous regions," *Engineering Fracture Mechanics*, vol. 19, no. 3, pp. 481–506, 1984.
- [5] N. Barton, "Some size dependent properties of joints and faults," *Geophysical Research Letters*, vol. 8, no. 7, pp. 667–670, 1981.
- [6] E. F. Glynn, D. Veneziano, and H. H. Einstein, *The Probabilistic Model For Shearing Resistance Of Jointed Rock*, American Rock Mechanics Association, 1978.
- [7] W. Nie, W. Wang, Z. Tao, C. Zhu, and Y. Chen, "Numerical modeling of the NPR-Cable and its applications for analysis of a slide-toe-toppling failure," *Computers and Geotechnics*, vol. 149, September, p. 104852, 2022.
- [8] M. He, Q. Sui, M. Li, Z. Wang, and Z. Tao, "Compensation excavation method control for large deformation disaster of mountain soft rock tunnel," *International Journal of Mining Science and Technology*, vol. 32, no. 5, pp. 951–963, 2022.
- [9] Y. Bao, J. Chen, L. Su, W. Zhang, and J. Zhan, "A novel numerical approach for rock slide blocking river based on the CEFDEM model: A case study from the Samaoding Paleolandslide blocking river event," *Engineering Geology*, vol. 312, January, p. 106949, 2023.
- [10] M. Shinozuka, "Basic analysis of structural safety," *Journal of Structural Engineering*, vol. 109, no. 3, pp. 721–740, 1983.
- [11] W. S. Dershowitz and H. H. Einstein, "Characterizing rock joint geometry with joint system models," *Rock Mechanics and Rock Engineering*, vol. 21, no. 1, pp. 21–51, 1988.
- [12] J. Zheng, J. Guo, J. Wang, H. Sun, J. Deng, and Q. Lv, "A universal elliptical disc (UED) model to represent natural rock fractures," *International Journal of Mining Science and Technology*, vol. 32, no. 2, pp. 261–270, 2022.
- [13] J. Guo, J. Zheng, Q. Lü, and J. Deng, "Estimation of fracture size and azimuth in the universal elliptical disc model based on trace information," *Journal of Rock Mechanics and Geotechnical Engineering*, vol. 15, no. 6, pp. 1391–1405, 2023.
- [14] Z. Tao, Q. Geng, C. Zhu, et al., "The mechanical mechanism of large-scale toppling failure for counter-inclined rock slopes," *Journal of Geophysics and Engineering*, vol. 16, no. 3, pp. 541–558, 2019.
- [15] S. Song, M. Zhao, C. Zhu, et al., "Identification of the potential critical slip surface for fractured rock slope using the Floyd algorithm," *Remote Sensing*, vol. 14, no. 5, p. 1284, 2022.
- [16] J. J. Song, "Estimation of a joint diameter distribution by an implicit scheme and interpolation technique," *International Journal of Rock Mechanics and Mining Sciences*, vol. 43, no. 4, pp. 512–519, 2006.
- [17] H. Zhu, Y. Zuo, X. Li, J. Deng, and X. Zhuang, "Estimation of the fracture diameter distributions using the maximum entropy principle," *International Journal of Rock Mechanics and Mining Sciences*, vol. 72, December, pp. 127–137, 2014.
- [18] Q. Zhang, Q. Wang, J. Chen, Y. Li, and Y. Ruan, "Estimation of mean trace length by setting Scanlines in rectangular sampling window," *International Journal of Rock Mechanics and Mining Sciences*, vol. 84, April, pp. 74–79, 2016.
- [19] M. Mauldon, "Estimating mean fracture trace length and density from observations in convex windows," *Rock Mechanics and Rock Engineering*, vol. 31, no. 4, pp. 201–216, 1998.

- [20] S. D. Priest and J. A. Hudson, "Estimation of discontinuity spacing and trace length using Scanlinesurveys," *International Journal of Rock Mechanics and Mining Sciences & Geomechanics Abstracts*, vol. 18, no. 3, pp. 183–197, 1981.
- [21] D. M. Cruden, "Describing the size of Discontinuities," *International Journal of Rock Mechanics and Mining Sciences & Geomechanics Abstracts*, vol. 14, no. 3, pp. 133–137, 1977.
- [22] P. H. S. W. Kulatilake and T. H. Wu, "Estimation of mean trace length of Discontinuities," *Rock Mechanics and Rock Engineering*, vol. 17, no. 4, pp. 215–232, 1984.
- [23] P. J. Pahl, "Estimating the mean length of discontinuity traces," *International Journal of Rock Mechanics and Mining Sciences & Geomechanics Abstracts*, vol. 18, no. 3, pp. 221–228, 1981.
- [24] M. Grenon and J. Hadjigeorgiou, "Drift reinforcement design based on discontinuity network modeling," *International Journal of Rock Mechanics and Mining Sciences*, vol. 40, no. 6, pp. 833–845, 2003.
- [25] Q. Wu, P. H. S. W. Kulatilake, and H. Tang, "Comparison of rock discontinuity mean trace length and density estimation methods using discontinuity data from an Outcrop in Wenchuan area, China," *Computers and Geotechnics*, vol. 38, no. 2, pp. 258–268, 2011.
- [26] S. D. Priest and J. A. Hudson, "Discontinuity spacings in rock," *International Journal of Rock Mechanics and Mining Sciences & Geomechanics Abstracts*, vol. 13, no. 5, pp. 135–148, 1976.
- [27] J. A. Hudson and S. D. Priest, "Discontinuities and rock mass geometry," *International Journal of Rock Mechanics and Mining Sciences & Geomechanics Abstracts*, vol. 16, no. 6, pp. 339–362, 1979.
- [28] X. Li, Y. Zuo, X. Zhuang, and H. Zhu, "Estimation of fracture trace length distributions using probability weighted moments and L-moments," *Engineering Geology*, vol. 168, no. 62, pp. 69–85, 2014.
- [29] L. Huang, H. Tang, L. Wang, and C. H. Juang, "Minimum Scanline-to-fracture angle and sample size required to produce a highly accurate estimate of the 3-D fracture orientation distribution," *Rock Mechanics and Rock Engineering*, vol. 52, no. 3, pp. 803–825, 2019.
- [30] A. Hekmatnejad, X. Emery, and D. Elmo, "A Geostatistical approach to estimating the parameters of a 3d Cox-Boolean discrete fracture network from 1D and 2d sampling observations," *International Journal of Rock Mechanics and Mining Sciences*, vol. 113, January, pp. 183–190, 2019.
- [31] N. H. Tran and S. S. Rahman, "Development of hot dry rocks by Hydraulic stimulation: Natural fracture network simulation," *Theoretical and Applied Fracture Mechanics*, vol. 47, no. 1, pp. 77–85, 2007.
- [32] L. Zhang and H. H. Einstein, "Estimating the mean trace length of rock Discontinuities," *Rock Mechanics and Rock Engineering*, vol. 31, no. 4, pp. 217–235, 1998.
- [33] Y. Zhang, J. Chen, F. Zhou, et al., "A novel approach to investigating 3d fracture Connectivity in Ultrahigh steep rock slopes," *International Journal of Rock Mechanics and Mining Sciences*, vol. 161, January, p. 105291, 2023.